Article

Zinc Oxide Nanoparticles and Fe-Modified Activated Carbon Affecting the In Vitro Growth of Date Palm Plantlets cv. Medjool

Yasmin M. R. Abdellatif [1], Maha S. Elsayed [2,*], Mona M. Hassan [2], Inas A. Ahmed [3,*], Ahmed H. Ragab [3], Ibrahim M. Shams El-Din [2], Walid B. Abdelaal [2], Mona S. Abd El-Aal [1] and Amal F. M. Zein El Din [2]

1　Department of Agricultural Botany, Faculty of Agriculture, Ain Shams University, Cairo 11566, Egypt
2　The Central Laboratory for Date Palm Researches and Development, Agricultural Research Center (ARC), Giza 12619, Egypt
3　Department of Chemistry, Faculty of Science, King Khalid University, Abha 62224, Saudi Arabia
*　Correspondence: maha.sobhy@arc.sci.eg or mahasobhy1000@yahoo.com (M.S.E.); eaahmed@kku.edu.sa (I.A.A.)

Abstract: The survival and growth of in vitro plantlets are still problematic for the date palm; thus, the application of nanotechnology may provide date palm plantlets that develop faster with enhanced growth and biochemical parameters. Moreover, the usage of Fe-modified activated carbon (Fe-AC) prepared from date palm pits instead of activated charcoal (AC) in tissue culture media during the current investigation can be considered an innovative approach. Furthermore, the effect of zinc oxide nanoparticles (ZnO-NPs) and bulk particles (ZnO-BPs) on the rooting and growth of date palm plantlets and on some physiological indices was also investigated. X-ray diffraction, dynamic light scattering, scanning electron microscopy, and transmission electron microscopy were used to characterize Fe-AC and ZnO-NPs. As detected from the characterization, the particle size was 720 nm for Fe-AC and 60 nm for ZnO-NPs. The obtained results indicated that AC significantly enhanced plantlet growth, plantlet height, number of leaves/plantlet, root length, number of roots/plantlet, and the concentrations of IAA, chlorophyll a and chlorophyll b compared with Fe-AC. On the other hand, sugars and phenols concentrations, and POD and PAL activities were highly increased with Fe-AC. There was no significant difference in terms of plant fresh weight (FW), leaf length, leaf width, protein, amino acids, and carotenoids. ZnO nanoparticles significantly improved plant height, leaf length, leaf width, root length, and the concentrations of IAA, chlorophylls a and b, and carotenoids; in contrast, the bulk form increased roots/plantlet, amino acids, and total sugars. Supplying the MS medium with combinations of ZnO-NPs or ZnO-BPs and AC or Fe-AC significantly increased all growth and physiological parameters. Plant height, leaf length, leaf width, root length, and the concentrations of IAA, protein, and chlorophylls a and b significantly increased when ZnO-NPs were combined with AC. Amino acids, total sugars, carotenoids, and phenols concentrations and the activities of POD and PAL increased when ZnO-BPs and Fe-AC were added together.

Keywords: *Phoenix dactylifera* L.; activated carbon; zinc oxide nanoparticles; zinc oxide bulk particles; growth; physiological response

1. Introduction

Date palm (*Phoenix dactylifera* L.) is a monocotyledonous, dioecious plant of the *Arecaceae* family. It is regarded as one of the most significant fruits harvested worldwide, especially in the Middle East, with over 14 million date palm trees; it is regarded as Egypt's primary crop and produces about 650,000 tons of dry matter per year [1]. Dates are utilized for both nutritional and phototherapeutic purposes, with effects against a wide range of diseases. Date fruits contain a variety of minerals, including potassium, calcium, magnesium, and phosphorus, as well as alkaloids, protein, carbohydrate, fatty acids (linoleic,

lauric, palmitic, and stearic acid), carotenoids, vitamins, and polyphenolic compounds. This variety of phytochemicals present confers a stronger impact on human health. Dates have a significant antioxidant capacity and are currently suggested as a potential source for various unique industrial and medical items [2]. Furthermore, dates show anticancer activity against a variety of cells due to the presence of phenolic compounds such as rutin and caffeic acid [3].

Recently, there has been increased interest in tissue-cultured date palm plants because a large number of uniform plants can be grown, which are true to type, disease-free, and scalable. Moreover, plant tissue culture, a significant biotechnology application, is a crucial tool for vegetative propagation and genetic alteration [4].

However, date palm micropropagation faces serious challenges due to the poor survival rate and the slow growth rate of the surviving tissue culture-derived date palm plantlets after acclimatization [5]. Thus, treatments that promote plantlet growth during in vitro rooting and hardening periods are urgently needed. Furthermore, in order for effective transplantation ex vitro, regenerated plantlets must be vigorous enough to overcome problems associated with the greenhouse [6].

Nanotechnology has become a cutting-edge innovation for scientific elaboration, and there has been increased interest in the usage of new nanomaterials in different fields such as industry and agriculture [7]. In the field of agriculture, several studies have used nanomaterials as micronutrient fertilizers for plants to regulate living processes at the cellular, tissue, and organ levels. A lack of these elements is unfavorable for plant growth and development [8]

One of the necessary micronutrients for plants is zinc, which is involved in a variety of physiological activities, including the activation of many enzymes and transcription factors, cellular metabolism, photosynthetic processes, plant cell division, cellular repair, and defensive mechanisms [9]. Variations in the concentration of zinc ions in plant cells may have a negative impact on plant development, stress tolerance, and chlorophyll production [10,11]. On the other hand, a more appropriate zinc concentration can increase the production of auxin and enhance plant development in general [12].

Inorganic (metal and metal oxide)-based zinc oxide nanoparticles (ZnO-NPs) are regarded among the most commonly used nanomaterials in the world [13]. Additionally, ZnO-NPs are crucial for the in vitro proliferation of date palms. The growth properties could be improved by using specific concentrations of ZnO-NPs in the culture medium [14].

Zinc increases the biosynthesis of auxin and gibberellins [15]. This increase in endogenous auxin can induce plumule growth and increase dry weight. Furthermore, the most significant functions of Zn^{2+} in chloroplast development and operation are the Zn-dependent activity of stromal processing peptidase and the repair of photosystem II (PSII) through the turnover of photodamaged D1 protein [16].

Plants require Zn^{2+} ions directly for tryptophan synthesis and indirectly for auxin synthesis [12]. The root process involves a number of physiological adjustments linked to differences in indole-3-acetic acid (IAA) concentration and peroxidase activity [17,18]. During this process, it was discovered that auxin concentration and peroxidase activity are inversely correlated [15,19,20]. Peroxidases play a crucial role in the IAA decarboxylation pathway, as extensively researched in the literature [21]. Plants that grow roots more quickly have increased peroxidase activity, according to Quoirin et al. [22]. Additionally, a positive correlation between the number of roots generated and the basic peroxidase activity has been found [23].

Activated carbons (AC) are materials characterized by a high surface area, a great number of pores, and various functional groups [24]. Therefore, they can be used in several applications: for gas separation, in supercapacitor electrodes, as catalyst support, and for the removal of organic and inorganic pollutants from wastewater. The production of AC is costly; thus, many researchers have sought to obtain low-cost alternatives to activated carbon from byproducts such as date palm pits [24], biopolymers [25], and coal [26]. The starting material, activation process, type of activating agent, and preparation

conditions, including temperature and activation time, all affect the textural characteristics and adsorption capacities of the produced AC [27].

AC is used in plant tissue culture to enhance cell formation and growth. It is characterized by the adsorption of inhibitory substances in the culture medium, a drastic decrease in the phenolic oxidation or brown exudate accumulation, adjusting the pH of the medium to an ideal level for morphogenesis, and the establishment of a darkened environment in the medium [28].

Chemical or physical activation processes can be used to prepare activated carbon from by-products. In case of chemical activation, we should use an activating agent such as $FeCl_3$, $ZnCl_2$, KOH, NaOH, or H_3PO_4. Ferric chloride as a chemical activating agent has some advantages with respect to other more traditional chemical activation agents. For example, it has a lower cost and is more environmentally friendly. Other traditional activating agents, such as KOH, NaOH, or H_3PO_4, are very strong bases and acids. The handling of these materials requires stricter security measures and materials more resistant to corrosion, increasing the cost of the synthesis process. All these facts mean that $FeCl_3$ activation can be considered low-cost and environmentally benign in comparison to those traditional activating agents [29].

Here, for the first time, is proof that the usage of Fe-AC from date palm pits in the field of tissue culture is being applied in a novel manner and inexpensive precursor for the production of Fe-activated carbon. Moreover, the production of activated carbon from date palm pits enables us to eliminate a considerable quantity of pits that are problematic in pastry factories.

The current study aimed to investigate the impact of using zinc oxide nanoparticles (ZnO-NPs) and Fe-modified activated carbon (Fe-AC) on the growth and rooting of date palm plantlets cv. Medjool. A good understanding of the physiological events related to the rooting stage such as evaluation of some biochemical constituents and some antioxidant enzyme activities.

2. Materials and Methods

2.1. Materials

Date palm pits were collected from a pastry factory in Cairo, Egypt, then washed to remove any contaminants, dried at 105 °C, and ground into fine particles. Zinc chloride, ferric chloride, sodium hydroxide, and zinc acetate were purchased from Sigma-Aldrich Co., St. Louis, MO, USA. All chemicals were used without further purification.

2.2. Methods

2.2.1. Preparation of Activated Carbon

Activated carbon obtained from date palm pits was prepared by drenching the pits in $ZnCl_2$ by a ratio of 1:3 (date palm pits: $ZnCl_2$) using a suitable amount of water. Then, the mixture was dried at 100 °C overnight. The last dried mixture was carbonized for 3 h in a stainless reactor (60 × 4 cm) at a rate of 10 °C/min up to 550 °C. The prepared sample was washed with deionized water to remove zinc cations, then dried.

2.2.2. Preparation of Fe-Modified Activated Carbon (Fe-AC)

Fe-AC was prepared by mixing 2 g of the previously activated carbon prepared from date palm pits with 200 mL of a 200 mg/L ferric chloride solution for 24 h; then, the solid was filtered, washed, and dried at 80 °C for 24 h.

2.2.3. Preparation of Zinc Oxide Nanoparticles (ZnO-NPs)

Zinc acetate dehydrate [Zn $(CH_3COO)_2$. $2H_2O$] and sodium hydroxide (NaOH) were dissolved in deionized water to form 0.05 M of zinc acetate and 0.1 M of NaOH. Droplets of sodium hydroxide were added to the zinc acetate under stirring at 50 °C till the formation of a transparent white solution; then, the samples were aged in an oven for 2 h at 90 °C.

The solution was centrifuged at 4000 rpm for 10 min. Then, the precipitate was washed several times, dried, ground in mortar, and calcined at 500 °C to obtain nano zinc oxide.

2.3. Characterization of Fe-Modified Activated Carbon and Zinc Oxide Nanoparticles

Different techniques were used for the characterization of Fe-AC and ZnO-NPs. X-ray diffraction patterns (XRD) were investigated using the PANalytical (Netherland) Model: X'PertPRO (MPD). Dynamic Light Scattering (DLS), including zeta potentials and particle size distributions (DLS), were determined using Zetasizer Nano (Nano ZS, Malvern, UK). The Fe-AC sample was characterized using a scanning electron microscope (SEM) (Quanta 250 FEG), while a ZnO-NPs sample was studied via HR-TEM (JEOL, JEM-2100, Tokyo, Japan). The surface area was determined using the (Microtrac BELSORP, Osaka, Japan) technique. Before the measurement and determination of adsorption-desorption isotherms, the samples were degassed under a vacuum at 180°C overnight.

2.4. Plant Material and Growth Conditions

The study was conducted in the tissue culture lab of the Central Laboratory for Date Palm Researches and Development, Agricultural Research Center (ARC), Giza, Egypt, and the Plant Physiology lab of the Agricultural Botany Department, Faculty of Agriculture, Ain Shams University, Egypt during the period of 2020–2022. The date palm cv. Medjool (eighteen-week-old plantlets) was used in this investigation (this period started from culturing the germinated somatic embryos on a culture medium that contained 0.2 mg/L of paclobutrazol (PBZ) for three subcultures to obtain healthy shoots for the rooting stage). The uniform plantlets were cultured on half-strength (MS) Murashige and Skoog [30] medium supplemented with naphthalene acetic acid (NAA) at 0.1 mg/L and sucrose at 10 g/L. Six treatments were applied as the following: no ZnO and 0.1 g/L activated charcoal (AC: activated charcoal, which is often used in tissue culture); no ZnO and 0.1 g/L Fe-AC; 10 mg/L zinc oxide nanoparticles (ZnO-NPs) plus 0.1 g/L AC; 10 mg/L ZnO-NPs plus 0.1 g/L Fe-AC; 10 mg/L ZnO bulk (ZnO-BPs) plus 0.1 g/L AC; and 10 mg/L ZnO-BPs plus 0.1 g/L Fe-AC. The treatments performed under the investigation at present occurred in two steps: during the first step (6 weeks), 6 g/L agar was used to solidify the culture media to induce the formation of roots, and during the second step (4 weeks), plantlets were placed into the liquid culture media to encourage the development of a strong root system. Five plantlets for each treatment were utilized. The size of the culture tube was 18 cm in length and 2.5 cm in width. The pH was adjusted to 5.7–5.8 during the first step and 5.2–5.3 during the second step, and all culture media were then autoclaved at 120°C for 15 min. The culture conditions were the same as those described by Zein El Din et al. [6].

2.5. Morphological Characteristics

The morphological data were recorded as follows: growth vigor, plantlet fresh weight (g), plantlet height (cm), number of leaves/plantlets, leaf length (cm), leaf width (cm), root length (cm), and number of roots/plantlets. The growth vigor was obtained visually as degrees according to Pottino [31].

2.6. Physiological and Biochemical Analyses

2.6.1. Assessment of Indole Acetic Acid

Indole acetic acid (IAA) was extracted and determined by Salkowski reagent according to the method of Shindy and Smith [32]. IAA was calculated as mg/g FW.

2.6.2. Assessment of Photosynthetic Pigments

Photosynthetic pigments (chlorophyll a, chlorophyll b, and carotenoids) were estimated in the ethanolic extract at 95% and calculated as mg/g FW according to Sumanta [33].

2.6.3. Assessment of Total Soluble Phenolic Compounds

Total soluble phenolic compounds were determined by the Folin–Ciocalteu colorimetric method described by Shahidi and Naczk [34]. Gallic acid was used as a standard and the total phenols concentration was expressed as mg/g FW.

2.6.4. Assessment of Free Amino Acids

Free amino acids were calorimetrically measured by using ninhydrin according to Jayeraman [35] and expressed as mg/g FW using glycine as a standard.

2.6.5. Assessment of Total Soluble Sugars

Total soluble sugars were estimated by 3,5-dinitro salicylic acid according to the method of Miller [36] using glucose as a standard. Soluble sugars were expressed as mg/g FW.

2.6.6. Assessment of Soluble Protein

Protein concentration was quantified in the crude enzyme extract as the method of Bradford [37] and expressed as mg/g FW. Bovine serum albumin was used as a standard.

The leaves were gently homogenized with a potassium phosphate buffer (pH = 7) containing 1% polyvinyl pyrrolidone and 0.1 mM EDTA. Supernatants were used as enzyme crude extracts to estimate the specific activity of guaiacol peroxidase (POD) and phenylalanine ammonia lyase (PAL) using a UV–Vis spectrophotometer UV 9100 B, LabTech.

2.6.7. Assay of Peroxidase Activity (POD)

POD (E.C 1.11.1.7) activity was determined according to the method of Hammer Schmidt et al. [38] and calculated by tracking the change in the absorbance at 470 nm per min unit of enzyme and expressed as unit/mg protein.

2.6.8. Assay of Phenylalanine Ammonia Lyase Activity (PAL)

PAL (E.C 4.3.1.5) activity was estimated according to the method of Lister et al. [39] who considered that each unit of enzyme activity was defined as the amount of enzyme that caused an increase in the absorbance of 0.01 per hour at 290 nm and expressed as unit/mg protein.

2.7. Statistical Analysis

SAS [40] software was performed using the two-way ANOVA technique. Five replicates were utilized to calculate the means, and the significant differences between the means were compared using Tukey's Studentized Range (HSD) test at $p \leq 0.05$.

3. Results

### *3.1. X-ray Diffraction (XRD)*

XRD is one of the techniques commonly used for structural characterizations. A normal-focus (PANalytical, Netherland diffractometer) source Cu target at 40 kV and 40 mA was used. The data were recorded in the range of 5–80θ. Figure 1a represents the XRD of the Fe-AC sample after the washing step, showing broad peaks around 25° and 43°; these peaks are typically characteristic of (002) and (100) planes of carbon [41]. The XRD of the ZnO-NP sample showed 2θ values at 31.84°, 34.52°, 36.38°, 47.64°, 56.7°, 63.06°, 68.1°, and 69.18° as presented in Figure 1b. All evident peaks could be indexed as a zinc oxide wurtzite structure (JCPDS Data Card No: 36-1451).
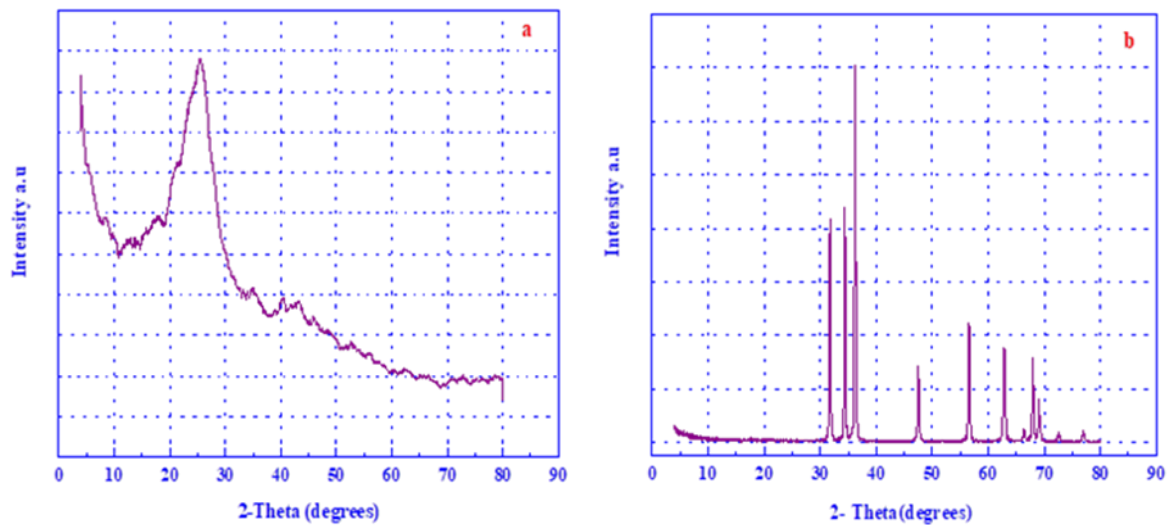
Figure 1. XRD diffractogram of synthesized (**a**) Fe-AC; (**b**) ZnO-NPs samples.

3.2. Dynamic Light Scattering (DLS)

This is a widely used technique for the determination of particle size in a colloidal solution. The samples were homogenized with ethanol and subsequently analyzed through a zeta nanosizer at room temperature. Figure 2a shows that the size distribution of the Fe-AC sample is 720 nm, while the size distribution of the ZnO-NP sample is 60 nm, as represented in Figure 2b.
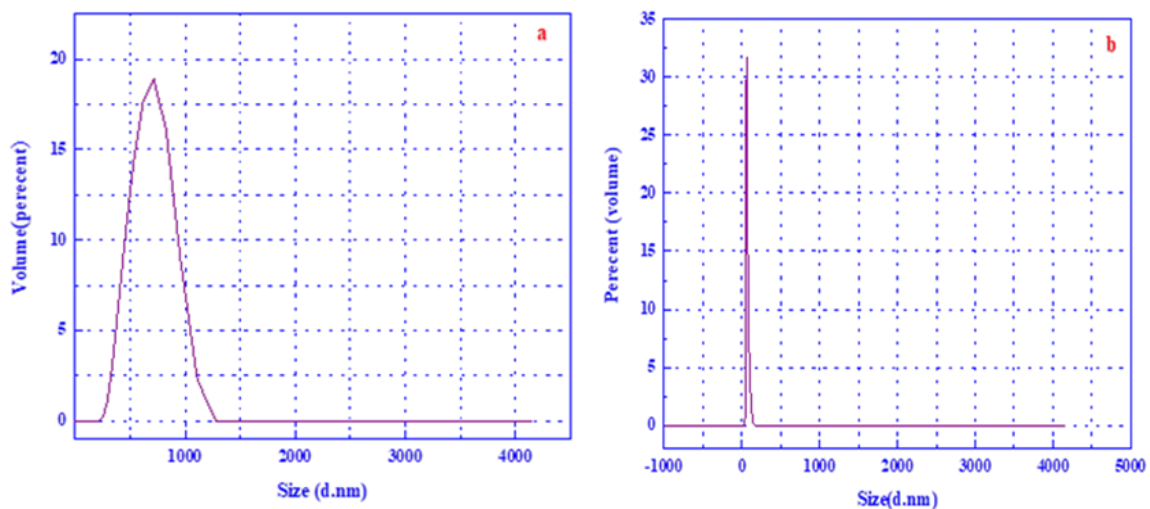
Figure 2. Particle size distribution of synthesized (**a**) Fe-AC; (**b**) ZnO-NPs samples.

3.3. Zeta Potential Analysis

The value of the zeta potential provided an insinuation of the potential stability of particles present in the colloid solution. If the particles in a suspension present high negative or positive zeta potential value, particles will repel each other and there will be no accumulation of nanoparticles. However, if the particles have low zeta potential levels, there will be no force to prevent the particles from aggregating. In the current study, the zeta potential values of Fe-AC and ZnO-NPs were 43.6 and −34.9 mv, respectively (Figure 3a,b).
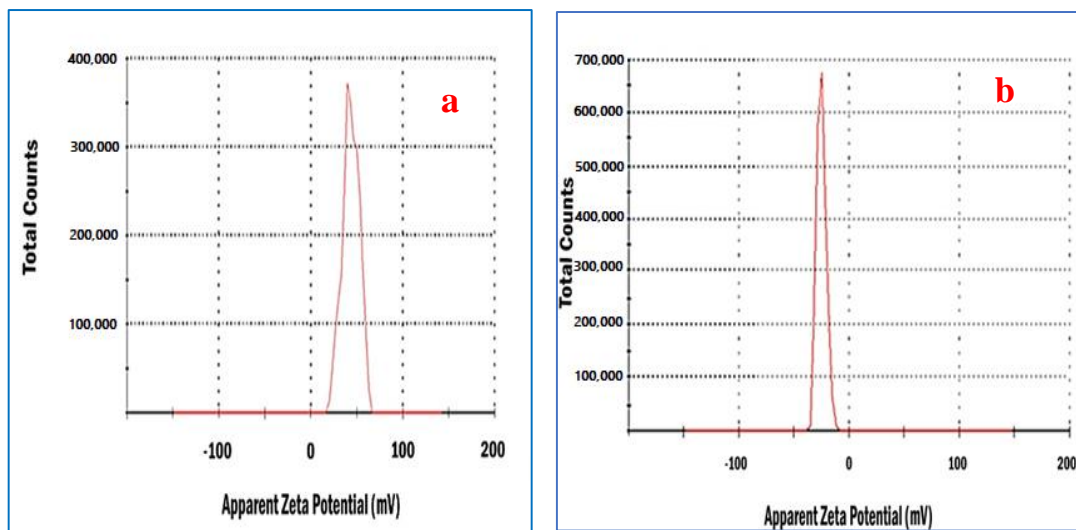
Figure 3. Zeta potential analysis of synthesized (**a**) Fe-AC; (**b**) ZnO−NPs samples.

*3.4. Scanning and Transmission Electron Microscopic Images*

The surface images of the Fe-AC sample were analyzed by scanning electron microscope (SEM), as shown in Figure 4a, which presents the pores on the surface of Fe-modified activated carbon, while the morphological characteristics of synthesized ZnO-NPs were studied via transmission electron microscopy (TEM), as shown in Figure 4b. The TEM image indicates that ZnO-NPs particles have a rod-like morphology.
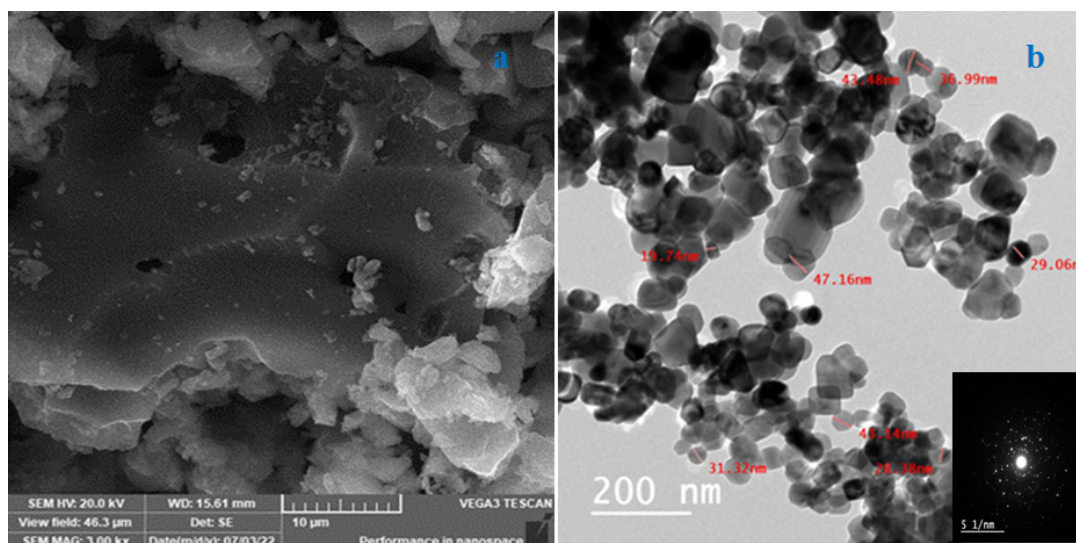
Figure 4. (**a**) Scanning electron microscopic image of Fe-AC; (**b**) transmission electron microscopic image of ZnO-NPs.

3.5. Surface Area

The adsorption-desorption isotherms at −196 °C for Fe-AC and ZnO-NPs are presented in Figure 5a,b. It is clear that the Fe-AC sample presents a hysteresis loop, also exhibiting a type-I adsorption isotherm, while ZnO-NPs produce an isotherm of type IV as mentioned by Li et al. [42]. Figure 5a,b was used to determine the specific surface area (S_{BET}, m^2/g), total pore volume (Vp, cm^3/g), and average pore radius ($\bar{r}$, nm). The BET surface area was determined by means of the standard BET equation applied in the relative pressure range from 0.05 to 0.30 [43], and the data are summarized in Table 1. The surface area of the Fe-AC sample was 369.75 m^2/g, while ZnO-NPs was 8.99 m^2/g.
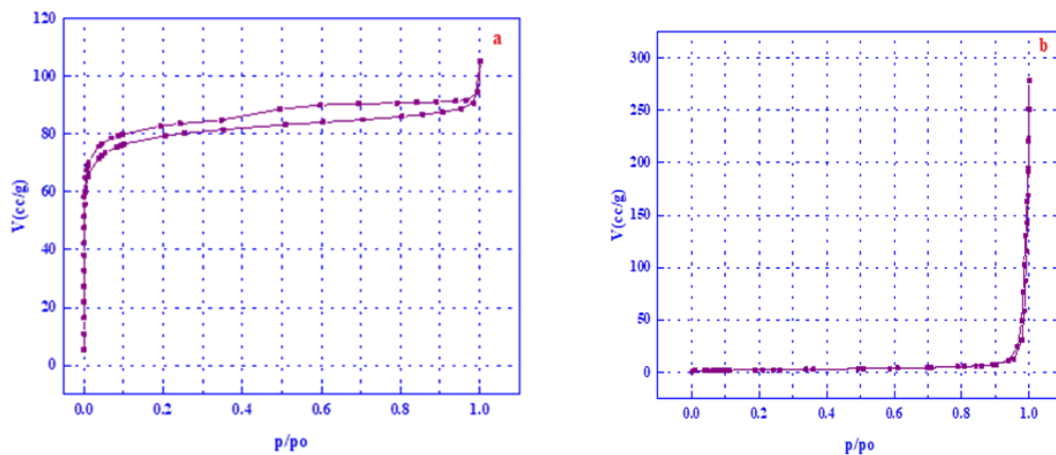
Figure 5. Nitrogen-adsorption isotherms of (**a**) Fe-AC and (**b**) ZnO-NPs samples at −196 °C.

Table 1. Textural properties of prepared samples from nitrogen adsorption at −196 °C.

Sample	S_{BET} (m^2/g)	C_{BET}	V_P (cm^3/g)	r (nm)
Fe-AC	369.75	2483	0.1470	1.9355
ZnO-NPs	8.99	102	0.1467	64.23

3.6. Morphological Observations

The data presented in Table 2 reveal that date palm plantlets cultured on medium supplemented with activated charcoal (AC) significantly stimulate greater growth vigor, plantlet height, number of leaves/plantlet, root length, and number of roots/plantlet than the plantlets cultured on medium supplemented with Fe-modified activated carbon prepared from date palm pits (Fe-AC), as shown in Figure 6a,b and Figure 7a,b, respectively. Insignificant differences were observed in the plantlets' fresh weight, leaf length, and leaf width between AC and Fe-AC treatments.
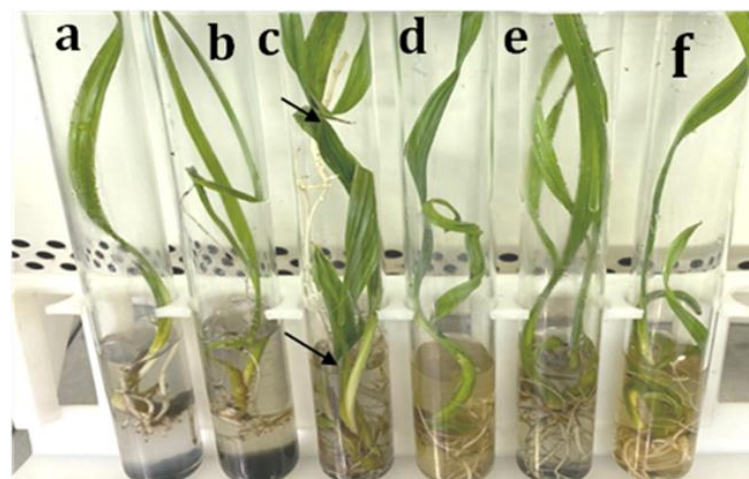
Figure 6. The influence of AC, Fe-AC, ZnO-NPs, and ZnO-BPs on the shoot and root growth, and development of date palm cv. Medjool; the treatments are added as follows: (**a**) no ZnO and 0.1 g/L AC; note the development of a few roots; (**b**) no ZnO and 0.1 g/L Fe-AC, treated plantlets are characterized by poor vigor and small leaf width; (**c**) 10 mg/L ZnO-NPs plus 0.1 g/L AC (the arrows point to the highest significant values of growth vigor, leaf width, number of leaves/plantlet, and root length); (**d**) 10 mg/L ZnO-NPs plus 0.1 g/L Fe-AC, note the high growth-rate vigor of grown plantlets; (**e**) 10 mg/L ZnO-BPs plus 0.1 g/L AC, treated plantlets are distinguished by the highest number of leaves/plantlet and roots/plantlet; (**f**) 10 mg/L ZnO-BPs plus 0.1 g/L Fe-AC, plantlets have a high number of roots/ plantlet. The plantlets were treated for 10 weeks.

Table 2. Effect of activated charcoal (AC), Fe-modified activated carbon (Fe-AC), zinc oxide nanoparticles (ZnO-NPs), and zinc oxide bulk particles (ZnO-BPs) and their combinations on some morphological parameters of date palm cv. Medjool grown in vitro. Five plantlets for each treatment were utilized for 10 weeks of treatment.

Treatments	Control	ZnO-NPs	ZnO-BPs	Mean	HSD	Control	ZnO-NPs	ZnO-BPs	Mean	HSD
	Growth vigor					**Plantlet fresh weight (g)**				
AC	2.33 [b] ± 0.58	5.00 [a] ± 0.00	5.00 [a] ± 0.00	4.11 [A]	0.40	0.72 [c] ± 0.01	2.54 [b] ± 0.02	2.50 [b] ± 0.05	1.92 [A]	0.14
Fe-AC	1.33 [c] ± 0.58	5.00 [a] ± 0.00	4.50 [a] ± 0.50	3.61 [B]		0.55 [c] ± 0.02	2.41 [b] ± 0.31	2.86 [a] ± 0.11	1.94 [A]	
Mean	1.83 [B]	5.00 [A]	4.75 [A]			0.63 [C]	2.48 [B]	2.68 [A]		
HSD		0.49					0.17			
	Plantlet height (cm)					**Number of leaves/plantlet**				
AC	27.67 [cd] ± 1.53	55.33 [a] ± 2.52	30.67 [c] ± 2.08	37.89 [A]	1.88	1.00 [b] ± 0.00	4.00 [a] ± 0.82	4.00 [a] ± 0.82	3.00 [A]	0.73
Fe-AC	25.33 [d] ± 0.58	36.67 [b] ± 2.08	29.67 [cd] ± 1.53	30.56 [B]		1.67 [b] ± 0.47	1.67 [b] ± 0.47	3.33 [a] ± 0.47	2.22 [B]	
Mean	26.50 [C]	46.00 [A]	30.17 [B]			1.33 [B]	2.83 [A]	3.67 [A]		
HSD		2.30					0.89			
	Leaf length (cm)					**Leaf width (cm)**				
AC	20.33 [d] ± 1.53	37.67 [a] ± 1.53	20.67 [d] ± 3.06	26.22 [A]	2.57	0.49 [c] ± 0.02	1.02 [a] ± 0.04	0.80 [b] ± 0.01	0.77 [A]	0.08
Fe-AC	15.50 [e] ± 0.50	31.00 [b] ± 4.58	25.67 [c] ± 1.53	24.06 [A]		0.30 [d] ± 0.02	1.08 [a] ± 0.16	0.82 [b] ± 0.07	0.73 [A]	
Mean	17.92 [C]	34.33 [A]	23.17 [B]			0.34 [C]	1.05 [A]	0.81 [B]		
HSD		3.15					0.09			
	Root length (cm)					**Number of roots/plantlet**				
AC	5.47 [c] ± 0.50	15.33 [a] ± 1.53	4.63 [cd] ± 0.65	8.48 [A]	0.88	3.33 [d] ± 0.58	14.67 [b] ± 1.53	18.33 [a] ± 1.53	12.11 [A]	1.33
Fe-AC	7.40 [b] ± 0.53	4.17 [cd] ± 1.04	3.13 [d] ± 0.15	4.90 [B]		2.33 [d] ± 0.58	11.33 [c] ± 1.53	16.33 [ab] ± 1.53	10.00 [B]	
Mean	6.43 [B]	9.75 [A]	3.88 [C]			2.83 [c]	13.00 [B]	17.33 [A]		
HSD		1.07					1.62			

According to Duncan's multiple range test at $p \leq 0.05$, the data show significant differences across treatments if the means are denoted by different letters. Capital letters represent means of AC, Fe-AC, and ZnO-NPs, ZnO-BPs treatments, whereas lowercase letters are used for interaction. Values are the means of five replicates ± SD.

The data presented in Table 2 also indicate that adding zinc oxide in the form of either nanoparticles (ZnO-NPs) or bulk particles (ZnO-BPs) significantly increases all the studied morphological parameters, except the root length, in comparison to the control plantlets. A significant increase in the plantlets' height was recorded with the application of ZnO-NPs (46.00 cm) followed by ZnO-BPs (30.17 cm) in comparison to the control (26.50 cm). The maximum increase in the leaf length, leaf width, and root length was also observed with ZnO-NPs being recorded at 34.33, 1.05, and 9.75 cm, respectively, whereas the maximum increase in the plantlets' fresh weight and the number of roots/plantlet (2.68 g and 17.33, respectively) were recorded with ZnO-BPs. Insignificant differences between ZnO-NPs and ZnO-BPs were recorded in the plantlets' growth vigor (5.00 and 4.75, respectively) and the number of leaves/plantlet (2. 83 and 3.67, respectively). Bulk particles of ZnO did not influence the length of the roots in comparison to the control, whereas it significantly increased with nanoparticles.

As illustrated in Table 2, the treatments with either ZnO-NPs or ZnO-BPs combined with AC or Fe-AC significantly increased all tested growth parameters in comparison to both control treatments (AC and Fe-AC). When ZnO-NPS were added to the medium supplemented with AC (Figures 6c and 7c), the plantlets' height, number of leaves/plantlet, leaf length, root length, and number of roots/plantlet considerably increased when compared to ZnO-NPS combined with Fe-AC (Figures 6d and 7d), whereas ZnO-BPs obtained the highest value for the number of roots/plantlet when combined with Fe-AC (18.33). The effects of nano or bulk ZnO combined with Fe-AC were more obvious with plantlet growth vigor. A significant increase in plantlet growth vigor was recorded with the combinations between ZnO-NPs or ZnO-BPs and AC or Fe-AC (5.00, 5.00, 5.00, and 4.50, respectively) in comparison to both control treatments (2.3 and 1.33), as presented in Figures 6e,f and 7e,f.
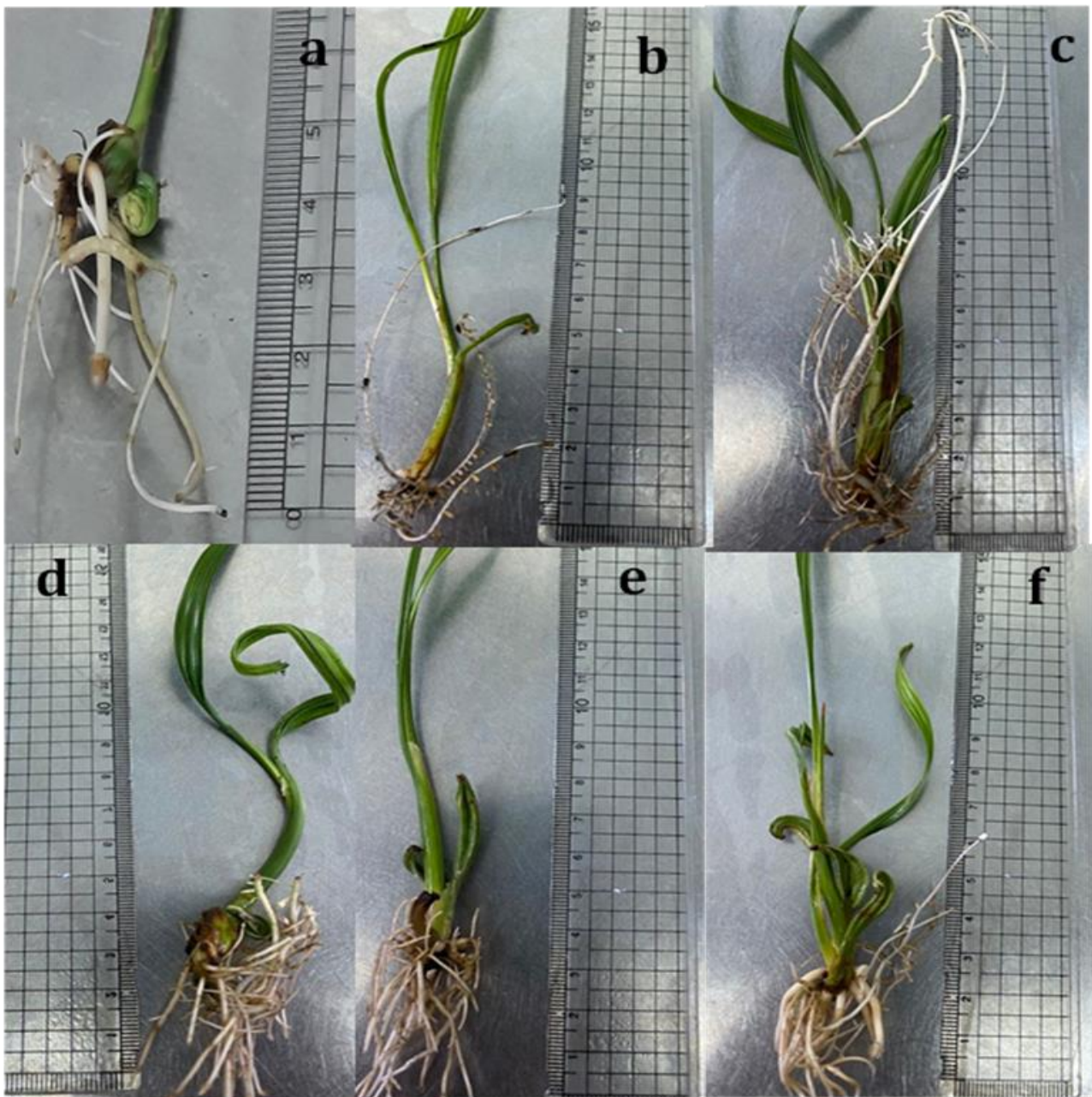
Figure 7. The influence of AC, Fe-AC, ZnO-NPs, and ZnO-BPs on root growth and development of date palm cv. Medjool; the treatments were supplemented as follows: (**a**) no ZnO and 0.1 g/L AC; (**b**) no ZnO and 0.1 g/L Fe-AC (note the poor development of the root system in both (**a**) and (**b**) as a result of the absence of ZnO from the culture media); (**c**) 10 mg/L ZnO-NPs plus 0.1 g/L AC (note the highest significant value of root length); (**d**) 10 mg/L ZnO-NPs plus 0.1 g/L Fe-AC; (**e**) 10 mg/L ZnO-BPs plus 0.1 g/L AC (note the highest significant values of the number of roots/plantlet); (**f**) 10 mg/L ZnO-BPs plus 0.1 g/L Fe-AC (note the good development of a root system in (**d**–**f**)). Plantlets were treated for 10 weeks.

3.7. Physiological Observations

Biochemical analyses were estimated as the concentrations of indole acetic acid (IAA), soluble protein, free amino acids, total sugars, chlorophyll a, chlorophyll b, carotenoids, and total soluble phenols, and the specific activities of guaiacol peroxidase (POD) and phenylalanine ammonia lyase (PAL) were also determined.

The results presented in Table 3 show that IAA significantly increases when AC is added to the media in comparison to Fe-AC. As for zinc oxide treatments, significant increases were detected with ZnO-NPs (0.079 mg/g FW) in comparison to ZnO-BPs (0.067 mg/g FW). Significant increases were detected when the media were supplied with ZnO-NPs combined with AC or Fe-AC.

Table 3. Effect of activated charcoal (AC), Fe-modified activated carbon (Fe-AC), zinc oxide nanoparticles (ZnO-NPs), and zinc oxide bulk particles (ZnO-BPs) and their combinations on some physiological parameters of date palm cv. Medjool grown in vitro. Five plantlets for each treatment were utilized for 10 weeks of treatment.

Treatments	Control	ZnO-NPs	ZnO-BPs	Mean	HSD	Control	ZnO-NPs	ZnO-BPs	Mean	HSD
	IAA (mg/g FW)					**Soluble Protein (mg/g FW)**				
AC	0.058 [c] ± 0.012	0.079 [a] ± 0.006	0.075 [ab] ± 0.006	0.073 [A]	0.008	0.04 [b] ± 0.006	0.07 [a] ± 0.024	0.05 [ab] ± 0.003	0.05 [A]	0.01
Fe-AC	0.057 [c] ± 0.004	0.077 [a] ± 0.003	0.064 [bc] ± 0.011	0.064 [B]		0.05 [ab] ± 0.013	0.06 [ab] ± 0.002	0.05 [ab] ± 0.015	0.05 [A]	
Mean	0.061 [B]	0.079 [A]	0.067 [B]			0.04 [A]	0.06 [A]	0.05 [A]		
HSD		0.009					0.02			
	Free amino acids (mg/g FW)					**Total sugars (mg/g FW)**				
AC	5.44 [cd] ± 1.11	6.29 [bc] ± 0.28	6.75 [ab] ± 0.70	6.16 [A]	0.65	1.50 [b] ± 0.16	1.87 [b] ± 0.25	1.72 [b] ± 0.11	1.69 [B]	0.32
Fe-AC	4.93 [d] ± 0.45	6.19 [bc] ± 0.28	7.70 [a] ± 0.55	6.28 [A]		1.42 [b] ± 0.08	1.65 [b] ± 0.08	3.09 [a] ± 0.69	2.05 [A]	
Mean	5.19 [C]	6.24 [B]	7.22 [A]			1.46 [B]	1.76 [B]	2.40 [A]		
HSD		0.79					0.3911			
	Chlorophyll a (mg/g FW)					**Chlorophyll b (mg/g FW)**				
AC	0.15 [d] ± 0.003	0.32 [a] ± 0.047	0.30 [ab] ± 0.002	0.26 [A]	0.02	0.12 [d] ± 0.004	0.19 [a] ± 0.020	0.18 [ab] ± 0.18	0.16 [A]	0.01
Fe-AC	0.17c [d] ± 0.007	0.27 [b] ± 0.008	0.20 [c] ± 0.019	0.21 [B]		0.13 [cd] ± 0.012	0.16 [ab] ± 0.008	0.15 [bc] ± 0.15	0.15 [B]	
Mean	0.16 [C]	0.30 [A]	0.249 [B]			0.13 [B]	0.17 [A]	0.17 [A]		
HSD		0.03					0.02			
	Carotenoids (mg/g FW)					**Total soluble phenols (mg/g FW)**				
AC	0.03 [b] ± 0.009	0.04 [ab] ± 0.006	0.04 [ab] ± 0.004	0.04 [A]	0.0056	1.03 [c] ± 0.31	1.50 [ac] ± 0.22	1.43 [bc] ± 0.006	1.32 [B]	0.40
Fe-AC	0.03 [ab] ± 0.001	0.04 [a] ± 0.004	0.03 [ab] ± 0.006	0.04 [A]		1.22 [bc] ± 0.08	1.79 [ab] ± 0.61	2.15 [a] ± 0.62	1.72 [A]	
Mean	0.03 [B]	0.04 [A]	0.04 [AB]			1.13 [B]	1.65 [A]	1.80 [A]		
HSD		0.007					0.49			
	POD (unit/mg protein)					**PAL (unit/mg protein)**				
AC	767.29 [d] ± 42.76	1172.38 [bc] ± 75.01	1274.93 [ac] ± 104.9	1071.53 [B]	115.64	353.49 [d] ± 82.2	806.37 [b] ± 53.51	676.87 [c] ± 38.74	612.24 [B]	65.09
Fe-AC	1075.92 [c] ± 41.5	1294.20 [ab] ± 198.65	1465.51 [a] ± 128.11	1278.54 [A]		574.88 [c] ± 12.52	833.67 [b] ± 103.70	971.66 [a] ± 45.60	793.39 [A]	
Mean	921.60 [B]	1233.29 [A]	1370.22 [A]			464.18 [B]	820.02 [A]	824.24 [A]		
HSD		141.63					79.73			

According to Duncan's multiple range test at $p \leq 0.05$, the data show significant differences across treatments if the means are denoted by different letters. Capital letters are used for means of AC, Fe-AC, and ZnO-NPs, and ZnO-BPs treatments, whereas lowercase letters are used for interactions. Values are the means of five replicates ± SD.

Regarding the concentrations of protein, amino acids, and carotenoids, insignificant differences were observed between AC and Fe-AC treatments. Meanwhile, significant increases in the total sugars and total soluble phenols were detected with the Fe-AC treatment when compared to AC. When AC was supplied to the media, both chlorophyll a and chlorophyll b contents were significantly stimulated in comparison to Fe-AC treatment. The authors detected that protein, chlorophyll a, chlorophyll b, and carotenoids increased with the treatment of ZnO-NPs followed by ZnO-BPs, while the lowest concentration was recorded with the control treatment. On the other hand, ZnO-BPs enhanced the concentrations of amino acids, total sugars, and total soluble phenols.

When the plantlets were cultured on media supplemented with ZnO-NPs combined with AC, protein, chlorophyll a, and chlorophyll b considerably increased (0.065, 0.325, and 0.185 mg/g FW, respectively). Meanwhile, the carotenoids' concentration increased with ZnO-NPs combined with Fe-AC (0.0433 mg/g FW). Concerning the plantlets that were cultured on the media amended with ZnO-BPs, the amino acids, total sugars, and total soluble phenols increased when Fe-AC was added.

The maximum activities of POD and PAL were shown with Fe-AC treatment in comparison to AC. Adding ZnO to the culture media increased the activities of POD and PAL antioxidant enzymes either in nano or bulk particles compared to the control treatment.

The data also revealed that the plantlets that were cultured on ZnO-BPs mixed with Fe-AC exhibited the greatest level of POD and PAL activities (1465.51 and 971.66 unit mg/g protein).

4. Discussion

According to the results of the XRD, the occurrence of weak and broad, noisy peaks at 2θ equal to 25 and 42 suggests that the structure of Fe-AC is particularly ordered as a part of the iron occupies the pores [44]. The abovementioned result is confirmed by the image produced by a scanning electron microscope, and it indicates that Fe-modified activated carbon is basically an amorphous solid. In the case of the ZnO-NPs sample, it represents a diffraction pattern consisting of a well-defined, narrow, sharp, and significant peak, which confirms that the sample is crystalline and free from impurities and does not contain any characteristic XRD peaks other than zinc oxide [45].

Figure 2 depicts a visualization of the particle sizes present in the solution. According to the results, a wider range of particles in the case of the Fe-AC sample can be explained by the thermal decomposition of biomass into smaller particles at high temperatures, followed by the clumping of some of these smaller particles into larger particles after cooling, and this result matches the results obtained by Siddique et al. [46]; on the other hand, the particle size of zinc oxide was 60 nm, which indicates that synthesized particles are of nanoscale and monodispersed. The latter data are in agreement with the transmission electron microscopy results.

It is generally considered that zeta potential values greater than +30 mV or less than −30 mV are thought to produce stable suspensions [47]. The zeta potential of the synthesized samples was determined in water as a dispersant; therefore, we observed that from the data, represented in Figure 3a, b, the Fe-AC sample has a zeta value of +43.6 mV; this means that the sample is stable in suspension. Moreover, ZnO-NPs have a zeta value of −34 mV; this high value confirms the repulsion among the particles and thereby increases the stability of the formulation [48] and prevents the particles from agglomerating into larger particle sizes.

From the SEM image of the Fe-AC sample, fewer pores are visible on the activated carbon surface as it is filled with ferric chloride. From the TEM image of ZnO-NPs, it can be indicated that the average particle size is in the range of 19–49 nm and this is in a good agreement with our previous results. The selected area's electron diffraction reveals the crystallization of the sample [49,50].

Nitrogen adsorption-desorption is represented in Figure 5a,b and indicates a hysteresis loop for the investigated Fe-AC sample; it is classified as type H4, which belongs to highly porous materials that can be related to the effect of pore connectivity [51]. The data presented in Table 1 suggest the surface area and microporous volume of the Fe-AC sample. Table 1 shows that S_{BET} and Vp are affected by the presence of ferric chloride in the sample, as ferric chloride has a relatively small ionic size and can enter the pores of activated carbon samples, which can also occupy some pores on the surface; therefore, the S_{BET} of Fe-AC is 369.75 m^2/g and the total pore volume is 0.1470 cm^3/g. The surface area of ZnO-NPs is 8.99m^2/g and affected by the condition of preparation. In this study, zinc acetate was used as the starting material and ZnO-NPs was prepared by the precipitation method at 50 °C and followed by the thermal treatment of these products at 500 °C. The effects of calcination temperatures indicated that 500 °C is the optimum calcination temperature to produce the ZnO nanoparticles with a favored surface area (8.99 m^2/g) and pore size (64.32 nm).

In the current study, the morphological growth parameters of date palm plantlets considerably varied depending on the in vitro cultured media. The obtained results indicate that the treatment of ZnO nanoparticles (ZnO-NPs) with the addition of activated charcoal (AC) exhibits the highest significant ($p \leq 0.05$) growth characters compared to the media fortified with a combination of ZnO-NPs and Fe-AC.

It is well-documented that activated charcoal is vital for promoting growth and organogenesis [52]. Sparjanbabu et al. [53] affirmed that AC induces greater plant growth and plant survival rates. They confirmed that AC reduces the browning of palm tissues and

culture media. Activated charcoal may be able to adsorb toxic pigments and phenolic compounds, as well as providing a suitable environment for seedling growth through their fine network of pores within larger inner surface areas, which inhibitory substances can adsorb [52].

As for the presence of Fe-AC in the media instead of AC, browning in the media was shown, which may have been due to the accumulation of polyphenolic compounds that indicate the low adsorption ability of Fe-AC due to its larger-sized particles. The accumulation of phenolic compounds in the culture media causes tissues to suffer from oxidation [54]. The oxidized exuded phenolics often block the uptake of required nutrients with consequences occurring from retarded growth resulting in death [55].

The inclusion of zinc oxide, especially ZnO-NPs, accelerates the superior values of all stages of date palm growth [14,56]. In this response, Sturikova et al. [9] reported that zinc is a member of the micronutrients group that has a nutritional value; it participates in protein binding, enzyme activity, and signal transduction in addition to acting as an enzyme cofactor. The medium supplemented with ZnO-NPs at doses of 6 and 18 mg/L increased the number of roots and shoots, the fresh and dry weights of olive plantlets [57], and also increased the shoot length and produced increased biomass in two pomegranates [58]. Furthermore, ZnO-NPs have greater solubility and improve the root's wheat uptake of excessive amounts of zinc [59] that diffuse in the extracellular spaces and increase the intracellular level of Zn^{2+} [60]. In this respect, Al-Mayahi [14] observed that the accumulation of elements (N, P, K, S, and Zn) in the date palm shoot developed in vitro was considerably impacted by ZnO-NPS treatments.

The primitive effect on the number of roots and root length that was clearly detected with the combination of AC and ZnO-NPs in the current study correlated to that of Pan and Van Staden [61] who reported that the presence of AC in the medium caused a decrease in the pH level. Acidic conditions can encourage rooting by accelerating the transfer of basipetal indole-3-acetic acid to the zone of root initiation [62]. Moreover, AC can provide a dark environment, keeping the light away from the rooting zone. IAA is hypothesized to be oxidized less rapidly in the dark than in the light [63]. IAA is a crucial component of root development, cell division, and the ability of cell walls for extension purposes [64]. Referring to ZnO-NPs, Zn is a cofactor in the pathway of IAA biosynthesis. A detectable increase in IAA was recorded in date palm shoots grown in vitro after ZnO-NPs treatment [14]. This increase may be attributed to the catalyzed role of Zn in the functioning of enzymes responsible for the conversion of tryptophan into IAA. Thus, it is clear that the addition of zinc oxide, specifically ZnO-NPs and AC or Fe-AC, accelerates the growth of more robust palm plantlets. Since more vigorous plantlets generate more efficient roots and have stronger growth potential, these factors are crucial for adaptation and transplanting processes under ex vitro circumstances [65].

Chlorophyll a and b are two crucial molecules that can be influenced and modulated by a wide range of variables. As for our study, the samples subjected to ZnO-NPs combined with AC presented higher levels of chlorophyll a and b in comparison to the other remaining treatments. When the plants are cultivated under normal conditions or under abiotic stress, such as salinity and exposure to heavy metals, nanomaterials in general and metal oxide nanoparticles, in particular, can affect the quantities of chlorophyll a and b [66,67]. This effect can be explained based on the role of zinc in chloroplast formation and development, as well as protochlorophyllide biosynthesis [68]. For instance, zinc is regarded as one of the minerals that is the most important for supporting the synthesis of chlorophylls [69]. The increase in chlorophylls is attributed to the capacity of ZnO-NPs to enhance photosynthetic efficiency by increasing chlorophyll's ability to absorb light. In particular, the mechanism causing this effect was the transfer of energy from ZnO-NPs to chlorophyll a, which in turn caused the pigment contents to increase [65].

Regarding the carotenoids present in the current study, ZnO, especially ZnO-NPs, enhanced the carotenoids' concentration. This result is in line with the results of Hassan et al. [56], who reported that the carotenoids' concentration increased significantly by adding ZnO-

NPs to the date palm shoots culture media. Carotenoids not only act as light-harvesting pigments, but they also have an important anti-oxidant protective function because of their capacity to eliminate reactive oxygen species [68,70]. Furthermore, carotenoids are able to quench chlorophylls in singlet and triplet forms to protect chloroplasts from oxidative damage [68]. The increase presented in our present study with the combination of ZnO-NPs and Fe-AC and the combination of ZnO-NPs and AC is noteworthy since it demonstrates how the application of NPs can enhance the light-harvesting ability and stress-resistance features of in vitro palm plantlets, hence promoting their growth.

The other parameter investigated in this experiment was the total soluble phenolic compound concentration; these biomolecules are considered another essential antioxidant similar to carotenoids [71]. In particular, phenols serve as oxygen radical scavengers as they have a lower electron reduction potential than oxygen radicals [72]. Several studies evidenced increases in phenols following ZnO treatment in date palm and *Brassica nigra* L. crops [56,73]. In a micro-propagated *study* on *Stevia rebaudiana*, the authors observed that there were inductive effects on the total phenolics at concentrations between 1.0 and 10 mg/L of ZnO-NPs [74]. According to the relevant literature, the increase in total phenols can be attributed to their ability to cope with metal cations. Moreover, in addition to the role of phenols as ROS scavengers, they also have the ability to chelate metals [72]. It is well known that the phenylpropanoid pathway, which produces phenolic acids primarily and monolignols subsequently, is first rate-limited by phenylalanine ammonia-lyase (PAL). It has been demonstrated that the binding state of peroxidase (POD) in the cell wall is related to the polymerization of monolignol and, consequently, the formation of lignin [75]. Secondarily thickened plant cell walls mostly comprise lignin as their structural base. Lignin provides mechanical support and facilitates the effective transport of water and solutes across long distances within the vascular systems [76].

Our results evidence an alleviated soluble protein concentration in the in vitro palm cultures due to the applied ZnO, particularly in the media amended with both ZnO-NPs and AC, whereas the amino acids and total sugars increased with ZnO-BPs fortified with Fe-AC. Zinc plays a role as a cofactor in numerous enzymes related to photosynthetic reactions and the metabolism of nucleic acids, proteins, and carbohydrates [9]. In line with these results, an investigation using biogenic ZnO-NPs derived from *Mentha arvensis* L. showed that these NPs improved various biochemical and nutritional characteristics, as well as increasing the soluble protein content in *Brassica napus* L. [77]. Zinc has a stimulatory effect on nutritional uptake and induces protein biosynthesis [14].

Higher soluble protein content was attributed to the protective action caused by these NPs, specifically to their ability in stimulating antioxidant enzyme activities [78]. The upshot of this impact is an increase in biomass output and plant growth [79]. As for amino acids and the total sugars increased with ZnO-BPs fortified with Fe-AC, it is suggested that Zn as a micro-element in addition to the high accumulation of phenolic compounds in the presence of large-sized particles of Fe-AC may be less effective at converting simple sugars into more complex carbohydrates or translocating sugars from leaves to other parts of plants [80]. Furthermore, it has been demonstrated that Zn ions encourage the synthesis of amino acids and peptides in plants [81]. The reason for the increase in the content of leaves from amino acids may be due to the vital role of zinc in the biosynthesis of tryptophan, which acts as a catalyst in the production of IAA [82]. They also added that small organic molecules, including amino acids and their derivatives, as well as simple sugars and their derivatives, are osmotically active molecules that preserve positive turgor pressure, which is necessary for the cell division and structural integrity of bio membranes. Moreover, it has been recommended that several endogenous amino acids play a crucial role in differentiation and morphogenesis [83].

Concerning Fe-AC that may enhance the accumulation of free amino acids and total sugars when combined with ZnO-BPs, our data may be explained by the fact that iron is largely required for chloroplasts, mitochondria, and peroxisomes to perform oxidation/reduction (redox) reactions. Iron is necessary for the synthesis of amino laevulinic

acid and protoporphyrinogen, which are the early and late precursors of chlorophyll, respectively. A deficit causes pronounced leaf chlorosis. Ferredoxin proteins, which serve as transporters of electrons during photosynthesis, contain iron as well [84].

Finally, our study investigated the specific activities of guaiacol peroxidase (POD) and phenylalanine ammonia-lyase (PAL) as antioxidant enzyme scavengers. The results obtained for POD- and PAL- specific activities are in line with those obtained for carotenoids and total soluble phenolic compounds. These results suggest that the levels of BPs and NPs applied in the current study encourage these enzymes in palm plantlets to survive ZnO stress. POD and PAL are regularly assessed as highlighted antioxidants that are active following their exposure to stress [85,86]. These results might point to the possibility of ZnO combining with the POD substrate complex [87]. Owing to these scientists, peroxidase activity has been linked to a variety of physiological functions of auxin and the synthesis of cell walls. Peroxidases use H_2O_2 to oxidize a variety of organic and inorganic substrates [88]. Guaiacol peroxidase utilizes guaiacol as an electron donor and participates in developmental processes and lignification as the same trend was observed for phenols. Lignin biosynthesis might build up a physical barrier to protect against excess poisonous heavy metals [89].

The data at present assumed that ZnO-BPs or ZnO-NPs treatments enhanced the PAL activity in date palm tissues. This result denotes that the PAL enzyme contributes to the production of secondary metabolites by enhancing the phenylpropanoid pathway in date palms, supporting antioxidant systems in response to elevated ROS, and increasing cell resistance to Zn stress. This may be related to the phenolic compounds increasing in plantlets cultured in media amended with ZnO-BPs and Fe-AC. Under ZnO-NP or BP treatments, the increment in the total phenolic compounds' concentration resulting from the activity of PAL can act as an electron transmitter that facilitates the transfer of electrons to ROS in the antioxidant system [90].

5. Conclusions

Date palm pits are taken into consideration as a novel and inexpensive precursor for the chemical synthesis of Fe-activated carbon. Additionally, the precipitation process is used to create zinc oxide nanoparticles from zinc acetate. Enhancing plantlet growth by supplying culture media with zinc oxide, particularly ZnO-NPs, in addition to AC and Fe-AC, may be advantageous for adaptation and transplanting processes under ex vitro circumstances since stronger plantlets have more potential and create more effective roots. Although this was the first time Fe-AC has been utilized in the date palm culture media, when Fe-AC substitutes AC, the browning of the medium was observed, which may have occurred due to the accumulation of polyphenolic compounds. However, Fe-AC treatment, especially when combined with ZnO-NPs, increased the carotenoid content. When Fe-AC was combined with ZnO-BPs, a significant increase in free amino acids, total sugars, and total phenols levels, and POD and PAL activities were evident. However, AC greatly enhanced plantlet height, number of leaves, leaf length, root length, and the concentrations of IAA, protein, and chlorophylls a, b when added to ZnO-NPs.

References

1. Kholif, A.E.; Gouda, G.A.; Patra, A.K. The sustainable mitigation of in vitro ruminal biogas emissions by ensiling date palm leaves and rice straw with lactic acid bacteria and *Pleurotus ostreatus* for cleaner livestock production. *J. Appl. Microbiol.* **2022**, *132*, 2925–2939. [CrossRef] [PubMed]

2. Qadir, A.; Shakeel, F.; Ali, A.; Faiyazuddin, M. Phototherapeutic potential and pharmaceutical impact of *Phoenix dactylifera* (date palm): Current research and future prospects. *J. Food Sci. Technol.* **2020**, *57*, 1191–1204. [CrossRef] [PubMed]

3. Mirza, M.B.; Elkady, A.; Al-Attar, A.M.; Syed, F.Q.; Mohammed, F.A.; Hakeem, K.R. Induction of apoptosis and cell cycle arrest by ethyl acetate fraction of *Phoenix dactylifera* L. (Ajwa dates) in prostate cancer cells. *J. Ethnopharmacol.* **2018**, *218*, 35–44. [CrossRef] [PubMed]

4. Kordrostami, M.; Mafakheri, M.; Al-Khayri, J.M. Date palm (*Phoenix dactylifera* L.) genetic improvement via biotechnological approaches. *Tree Genet. Genomes* **2022**, *18*, 1–28. [CrossRef]

5. Awad, M.A. Promotive effects of a 5-aminolevulinic acid-based fertilizer on growth of tissue culture-derived date palm plants (*Phoenix dactylifera* L.) during acclimatization. *Sci. Hortic.* **2008**, *118*, 48–52. [CrossRef]

6. Zein El Din, A.F.M.; Ibrahim, M.F.M.; Farag, R.; El-Gawad, H.; El-Banhawy, A.; Alaraidh, I.A.; Rashad, Y.M.; Lashin, I.; El-Yazied, A.A.; Elkelish, A.; et al. Influence of polyethylene glycol on leaf anatomy, stomatal behavior, water loss, and some physiological traits of date palm plantlets grown in vitro and ex vitro. *Plants* **2020**, *9*, 1440. [CrossRef]

7. Kasthuri, J.; Veerapandian, S.; Rajendiran, N. Biological synthesis of silver and gold nanoparticles using apiin as reducing agent. *Colloids Surf. B* **2009**, *68*, 55–60. [CrossRef] [PubMed]

8. Andresen, E.; Peiter, E.; Küpper, H. Trace metal metabolism in plants. *J. Exp. Bot.* **2018**, *69*, 909–954. [CrossRef]

9. Sturikova, H.; Krystofova, O.; Huska, D.; Adam, V. Zinc, zinc nanoparticles and plants. *J. Hazard. Mater.* **2018**, *349*, 101–110. [CrossRef]

10. Kawachi, M.; Kobae, Y.; Mori, H.; Tomioka, R.; Lee, Y.; Maeshima, M. A mutant strain *Arabidopsis thaliana* that lacks vacuolar membrane zinc transporter MTP1 revealed the latent tolerance to excessive zinc. *Plant Cell Physiol.* **2009**, *50*, 1156–1170. [CrossRef]

11. Lee, S.; Kim, S.A.; Lee, J.; Guerinot, M.L.; An, G. Zinc deficiency inducible osZIP8 encodes a plasma membrane-localized zinc transporter in rice. *Mol. Cells* **2010**, *29*, 551–558. [CrossRef] [PubMed]

12. Adhikari, T.; Kundu, S.; Rao, A.S. Zinc delivery to plants through seed coating with nano-zinc oxide particles. *J. Plant Nutr.* **2016**, *39*, 136–146. [CrossRef]

13. Rajput, V.; Minkina, T.; Sushkova, S.; Behal, A.; Maksimov, A.; Blicharska, E.; Ghazaryan, K.; Movsesyan, H.; Barsova, N. ZnO and CuO nanoparticles: A threat to soil organisms. *Environ. Geochem. Health* **2020**, *42*, 147–158. [CrossRef] [PubMed]

14. Al-Mayahi, A.M.W. The effect of humic acid (HA) and zinc oxide nanoparticles (ZnO-NPS) on in vitro regeneration of date palm (*Phoenix dactylifera* L.) cv. Quntar. *Plant Cell Tissue Organ Cult.* **2021**, *145*, 445–456. [CrossRef]

15. Cakmak, I. Enrichment of cereal grains with zinc: Agronomic or genetic biofortification. *Plant Soil* **2008**, *30*, 1–17. [CrossRef]

16. Hansch, R.; Mendel, R.R. Physiological functions of mineral micronutrients (Cu, Zn, Mn, Fe, Ni, Mo, B, Cl). *Curr. Opin. Plant Biol.* **2009**, *12*, 259–266. [CrossRef] [PubMed]

17. Hausman, J.F. Changes in peroxidase activity, auxin level and ethylene production during root formation by poplar shoots raised in vitro. *Plant Growth Regul.* **1993**, *13*, 263–268. [CrossRef]

18. Moncousin, C. Adventitious rhizogenesis control: New developments. *Acta Hortic.* **1988**, *230*, 97–104. [CrossRef]

19. Gendreau, E.; Traas, J.; Desnos, T.; Grandjean, O.; Caboche, M.; Hofte, H. Cellular basis of hypocotyl growth in *Arabidopsis thaliana*. *Plant Physiol.* **1997**, *114*, 295–305. [CrossRef]

20. Ripetti, V.; Kevers, C.; Gaspar, T. Two successive media for the rooting of walnut shoots in vitro. Changes in peroxidase activity and in ethylene production. *Adv. Hortic. Sci.* **1994**, *8*, 29–32.

21. Siegel, B. Plant peroxidases—An organismic perspective. *Plant Growth Regul.* **1993**, *12*, 303–312. [CrossRef]

22. Quoirin, M.; Boxus, P.; Gaspar, T. Root initiation and isoperoxidases of stem tip cuttings from mature *Prunus* plants. *Phys. Veg.* **1974**, *12*, 165–174.

23. De Klerk, G.J.; Ter Brugge, J.; Smulders, R.; Benschop, M. Basic peroxidases and rooting in microcuttings of Malus domestica. *Acta Hortic* **1990**, *280*, 29–36. [CrossRef]

24. Youssef, A.M.; El-Didamony, H.; El-Sharabasy, S.; Sobhy, M.; Hassan, A.F.; Buláneke, R. Adsorption of 2, 4 dichlorophenoxyacetic acid on different types of activated carbons-based date palm pits: Kinetic and thermodynamic studies. *Int. J. Pure Appl. Chem.* **2017**, *14*, 1–15. [CrossRef]

25. Marrakchi, F.; Ahmed, M.J.; Khanday, W.A.; Asif, M.; Hameed, B.H. Mesoporous activated carbon prepared from chitosan flakes via single-step sodium hydroxide activation for the adsorption of methylene blue. *Int. J. Biol. Macromol.* **2017**, *98*, 233–239. [CrossRef] [PubMed]

26. Gao, L.; Dong, F.Q.; Dai, Q.W.; Zhong, G.Q.; Halik, U.; Lee, D.J. Coal tar residues based activated carbon: Preparation and characterization. *J. Taiwan Inst. Chem. Eng.* **2016**, *63*, 166–169. [CrossRef]

27. Liu, Q.S.; Zheng, T.; Li, N.; Wang, P.; Abulikemu, G. Modification of bamboo-based activated carbon using microwave radiation and its effects on the adsorption of methylene blue. *Appl. Surf. Sci.* **2016**, *256*, 3309–3315. [CrossRef]

28. Thomas, T.D. The role of activated charcoal in plant tissue culture. *Biotechnol. Adv.* **2008**, *26*, 618–631. [CrossRef]

29. Bedia, J.; Peñas-Garzón, M.; Gómez-Avilés, A.; Rodriguez, J.J.; Belver, C. Review on activated carbons by chemical activation with $FeCl_3$. *J. Carbon Res.* **2020**, *6*, 21. [CrossRef]

30. Murashige, T.; Skoog, F. A Revised Medium for Rapid Growth and Bio Assays with Tobacco Tissue Cultures. *Physiol. Plant.* **1962**, *15*, 473–497. [CrossRef]

31. Pottino, B.G. *Methods in Plant Tissue Culture*; Deptartment of Horticulture, Agriculture College, Maryland University: College park, MD, USA, 1962; pp. 8–29.

32. Shindy, W.W.; Smith, O.E. Identification of plant hormones from cotton ovules. *Plant Physiol.* **1975**, *55*, 550–554. [CrossRef] [PubMed]

33. Sumanta, N.; Haque, C.I.; Nishika, J.; Suprakash, R. Spectrophotometric Analysis of Chlorophylls and Carotenoids from Commonly Grown Fern Species by Using Various Extracting Solvents. *Res. J. Chem. Sci.* **2014**, *4*, 63–69.

34. Shahidi, F.; Naczk, M. Methods of analysis and quantification of phenolic compounds. In *Food Phenolic: Sources, Chemistry, Effects and Applications*; Technomic Publishind Company, Inc.: Lancaster, PA, USA, 1995; pp. 287–293.

35. Jayeraman, J. *Laboratory Manual in Biochemistry*; Wiley Eastern Ltd.: New Delhi, India, 1985; p. 107.

36. Miller, G.L. Use of dinitrosalicylic acid reagent for determination of reducing sugar. *Anal. Chem.* **1959**, *31*, 426. [CrossRef]

37. Bradford, M.M. A rapid and sensitive method for the quantitation of microgram quantities of protein utilizing the principal of protein—Dye Binding. *Anal. Biochem.* **1976**, *72*, 248–254. [CrossRef] [PubMed]

38. Hammer Schmidt, R.; Nuckles, E.M.; Kuc, J. Association of enhanced peroxidase activity with induced systemic resistance of cucumber to *Colletotrichum lagenarium*. *Physiol. Plant.* **1982**, *20*, 73–82.

39. Lister, C.E.; Lancaster, J.E.; Walker, J.R.L. Phenylalanine ammonia-lyase activity and its relationship to anthocyanin and flavonoid levels in New Zealand grown apple cultivars. *J. Am. Soc. Hortic. Sci.* **1996**, *121*, 281–285. [CrossRef]

40. SAS. *SAS/STAT User's Guide, Release 6.03 ed.*; SAS Institute Inc.: Cary, NC, USA, 1988.

41. Xu, Z.; Zhang, T.; Yuan, Z.; Zhang, D.; Sun, Z.; Huang, Y.; Zhou, Y. Fabrication of cotton textile waste-based magnetic activated carbon using FeCl 3 activation by the Box–Behnken design: Optimization and characteristics. *RSC Adv.* **2018**, *8*, 38081–38090. [CrossRef] [PubMed]

42. Li, J.; Wang, Y.; Xu, W.; Wang, Y.; Zhang, B.; Luo, S.; Hu, C. Porous Fe_2O_3 nanospheres anchored on activated carbon cloth for high-performance symmetric supercapacitors. *Nano Energy* **2019**, *57*, 379–387. [CrossRef]

43. Aroua, M.K.; Leong, S.P.P.; Teo, L.Y.; Yin, C.Y.; Daud, W.M.A.W. Real-time determination of kinetics of adsorption of lead (II) onto palm shell-based activated carbon using ion selective electrode. *Bioresour. Technol.* **2008**, *99*, 5786–5792. [CrossRef]

44. Cheng, S.; Zhang, L.; Ma, A.; Xia, H.; Peng, J.; Li, C.; Shu, J. Comparison of activated carbon and iron/cerium modified activated carbon to remove methylene blue from wastewater. *J. Environ. Sci.* **2018**, *65*, 92–102. [CrossRef]

45. Bigdeli, F.; Morsali, A.; Retalleau, P. Synthesis and Characterization of Different zinc (II) Oxide Nano-Structures from Direct Thermal Decomposition of ID Coordination Polymers. *Polyhedron* **2010**, *29*, 801–806. [CrossRef]

46. Siddique, A.; Nayak, A.K.; Singh, J. Synthesis of $FeCl_3$-activated carbon derived from waste Citrus limetta peels for removal of fluoride: An eco-friendly approach for the treatment of groundwater and bio-waste collectively. *Groundw. Sustain. Dev.* **2020**, *10*, 100339. [CrossRef]

47. Meléndrez, M.F.; Cardenas, G.; Arbiol, J. Synthesis and Characterization of Gallium Colloidal Nanoparticles. *J. Colloid Interf. Sci.* **2010**, *346*, 279–287. [CrossRef] [PubMed]

48. Garcia, A.; Cuesta, A.; Montes-Moran, M.; Martinez-Alonso, A.; Tascon, J. Zeta Potential as a Tool to Characterize Plasma Oxidation of Carbon Fibers. *J. Colloid Interface Sci.* **1997**, *192*, 363–367. [CrossRef] [PubMed]

49. Elsayed, M.S.; Ahmed, I.A.; Bader, D.M.; Hassan, A.F. Green Synthesis of Nano Zinc Oxide/Nanohydroxyapatite Composites Using Date Palm Pits Extract and Eggshells: Adsorption and Photocatalytic Degradation of Methylene Blue. *Nanomaterials* **2021**, *12*, 49. [CrossRef]

50. Hassan, A.F. Synthesis of carbon nano-onion embedded metal–organic frameworks as an efficient adsorbent for cadmium ions: Kinetic and thermodynamic studies. *Environ. Sci. Pollut. Res.* **2019**, *26*, 24099–24111. [CrossRef]

51. Bulánek, R.; Hrdina, R.; Hassan, A.F. Preparation of polyvinylpyrrolidone modified nano magnetite for degradation of nicotine by heterogeneous Fenton process. *J. Environ. Chem. Eng.* **2019**, *7*, 102988–102996. [CrossRef]

52. Madhusudhanan, K.; Rahiman, B.A. The effect of activated charcoal supplemented media to browning of in vitro cultures of *Piper* species. *Biol. Plant.* **2000**, *43*, 297–299. [CrossRef]

53. Sparjanbabu, D.S.; Naveen Kumar, P.; Krishna, M.S.R.; Ramajayam, D.; Susanthi, B. Effect Of Activated Charcoal, Culture Media And Plant Growth Regulators on in Vitro Germination and Development of Elite Dura Oil Palm (*Elaeis guineensis* Jacq.) Zygotic Embryos. *Plant Cell Biotechnol. Mol. Biol.* **2019**, *20*, 314–323.

54. Cattelan, L.V.; Stein, V.C.; Souza, S.A.; Heiden, G.; Buttow, M.V.; Bobrowski, V.L. Estabelecimento in vitro de Matricaria recutita utilizando diferentes condicoes de cultivo. *Rev. Bras. Biociências* **2007**, *5*, 201–203.

55. He Guo, X.; Lu, R.; Niu, B.; Pasapula, V.; Hou, P.; Cai, F.; Xu, Y.; Chen, F. Changes in morphology and biochemical indices in browning callus derived from Jatropha curcus hypocotyls. *Plant Cell Tissue Organ Cult.* **2009**, *98*, 11–17. Available online: https://link.springer.com/article/10.1007/s11240-009-9533-y (accessed on 5 July 2022).

56. Hassan, M.M.; Taha, R.A.; Abd El-Aziz, M.E.; Shaaban, E.A.; Ibrahim, E.A. Impact of nano-zinc-oxide as an alternative source of zinc in date palm culture media. *Plant Cell Tissue Organ Cult.* **2022**, *150*, 73–84. [CrossRef]

57. Regni, L.; Del Buono, D.; Micheli, M.; Facchin, S.L.; Tolisano, C.; Proietti, P. Effects of Biogenic ZnO Nanoparticles on Growth, Physiological, Biochemical Traits and Antioxidants on Olive Tree In Vitro. *Horticulturae* **2022**, *8*, 161. [CrossRef]

58. El-Mahdy, M.T.; Elazab, D.S. Impact of Zinc Oxide Nanoparticles on Pomegranate Growth under In Vitro Conditions. *Russ. J. Plant Physiol.* **2020**, *67*, 162–167. [CrossRef]

59. Du, W.; Sun, Y.; Ji, R.; Zhu, J.; Wu, J.; Guo, H. TiO_2 and ZnO nanoparticles negatively affect wheat growth and soil enzyme activities in agricultural soil. *J. Environ. Monitor.* **2011**, *13*, 822–828. [CrossRef]

60. Pandurangan, M.; Kim, D.H. In vitro toxicity of zinc oxide nanoparticles: A review. *J. Nanoparticle Res.* **2015**, *17*, 158. [CrossRef]

61. Pan, M.; Van Staden, J. Effect of activated charcoal, autoclaving and culture media on sucrose hydrolysis. *Plant Growth Regul.* **1999**, *29*, 135–141. [CrossRef]

62. Liu, J.H.; Mukherjee, I.; Reid, D.M. Stimulation of adventitious rooting in sunflower (*Helianthus annuus*) by low pH: Possible role of auxin. *Can. J. Bot.* **1993**, *71*, 1645–1650. [CrossRef]

63. Norton, M.E.; Boe, A.A. In vitro propagation of ornamental Rosaceous plant. *HortScience* **1982**, *17*, 190–191. [CrossRef]

64. Spiegel-Roy, P.; Goldschmidt, E. *Biology of Citrus*; Cambridge University Press: Cambridge, UK; pp. 140–184.

65. Regni, L.; Micheli, M.; Del Pino, A.M.; Palmerini, C.A.; D'Amato, R.; Facchin, S.L.; Famiani, F.; Peruzzi, A.; Mairech, H.; Proietti, P. The First Evidence of the Beneficial Effects of Se-Supplementation on in Vitro Cultivated Olive Tree Explants. *Plants* **2021**, *10*, 1630. [CrossRef]

66. El-Saadony, M.T.; Desoky, E.-S.M.; Saad, A.M.; Eid, R.S.M.; Selem, E.; Elrys, A.S. Biological Silicon Nanoparticles Improve *Phaseolus vulgaris* L. Yield and Minimize Its Contaminant Contents on a Heavy Metals-Contaminated Saline Soil. *J. Environ. Sci. China* **2021**, *106*, 1–14. [CrossRef] [PubMed]

67. Manzoor, N.; Ahmed, T.; Noman, M.; Shahid, M.; Nazir, M.M.; Ali, L.; Alnusaire, T.S.; Li, B.; Schulin, R.; Wang, G. Iron Oxide Nanoparticles Ameliorated the Cadmium and Salinity Stresses in Wheat Plants, Facilitating Photosynthetic Pigments and Restricting Cadmium Uptake. *Sci. Total Environ.* **2021**, *769*, 145221. [CrossRef] [PubMed]

68. Del Buono, D.; Di Michele, A.; Costantino, F.; Trevisan, M.; Lucini, L. Biogenic Zno Nanoparticles Synthesized Using a Novel Plant Extract: Application to Enhance Physiological and Biochemical Traits in Maize. *Nanomaterials* **2021**, *11*, 1270. [CrossRef] [PubMed]

69. Salama, D.M.; Osman, S.A.; Abd El-Aziz, M.E.; Abd Elwahed, M.S.A.; Shaaban, E.A. Effect of Zinc Oxide Nanoparticles on the Growth, Genomic DNA, Production and the Quality of Common Dry Bean (*Phaseolus vulgaris*). *Biocatal. Agric. Biotechnol.* **2019**, *18*, 101083. [CrossRef]

70. Tedeschini, E.; Proietti, P.; Timorato, V.; D'Amato, R.; Nasini, L.; Dei Buono, D.; Businelli, D.; Frenguelli, G. Selenium as Stressor and Antioxidant Affects Pollen Performance in Olea Europaea. *Flora-Morphol. Distrib. Funct. Ecol. Plants* **2015**, *215*, 16–22. [CrossRef]

71. Dobrikova, A.G.; Apostolova, E.L.; Han´c, A.; Yotsova, E.; Borisova, P.; Sperdouli, I.; Adamakis, I.-D.S.; Moustakas, M. Cadmium Toxicity in *Salvia sclarea*, L.: An Integrative Response of Element Uptake, Oxidative Stress Markers, Leaf Structure and Photosynthesis. *Ecotoxicol. Environ. Saf.* **2021**, *209*, 111851. [CrossRef]

72. Salih, A.M.; Al-Qurainy, F.; Khan, S.; Tarroum, M.; Nadeem, M.; Shaikhaldein, H.O.; Gaafar, A.-R.Z.; Alfarraj, N.S. Biosynthesis of Zinc Oxide Nanoparticles Using *Phoenix dactylifera* and Their Effect on Biomass and Phytochemical Compounds in Juniperus Procera. *Sci. Rep.* **2021**, *11*, 19136. [CrossRef]

73. Zafar, H.; Abbasi, B.H.; Zia, M. Physiological and Antioxidative Response of *Brassica nigra* (L.) to ZnO Nanoparticles Grown in Culture Media and Soil. *Toxicol. Environ. Chem.* **2019**, *101*, 281–299. [CrossRef]

74. Javed, R.; Usman, M.; Yücesan, B.; Zia, M.; Gürel, E. Effect of Zinc Oxide (ZnO) Nanoparticles on Physiology and Steviol Glycosides Production in Micropropagated Shoots of Stevia Rebaudiana Bertoni. *Plant Physiol. Biochem.* **2017**, *110*, 94–99. [CrossRef]

75. Passardi, F.; Cosio, C.; Penel, C.; Dunand, C. Peroxidases have more functions than a Swiss army knife. *Cell Rep.* **2005**, *24*, 255–265. [CrossRef]

76. Deng, F.; Aoki, M.; Yogo, Y. Effect of naringenin on the growth and lignin biosynthesis of gramineous plants. *Weed Biol. Manag.* **2004**, *4*, 49–55. [CrossRef]

77. Sohail; Kamran, K.; Kemmerling, B.; Shutaywi, M.; Mashwani, Z.U.R. Nano zinc elicited biochemical characterization, nutrtitional assessment, antioxidant enzymes and fatty acids profiling of rapeseed. *PLoS ONE* **2020**, *15*, e0241568. [CrossRef] [PubMed]

78. Abdel-Wahab, D.A.; Othman, N.A.R.M.; Hamada, A.M. Zinc Oxide Nanoparticles Induce Changes in the Antioxidant Systems and Macromolecules in the Solanum Nigrum Callus. *Egypt. J. Bot.* **2020**, *60*, 503–517. [CrossRef]

79. El-Badri, A.M.A.; Batool, M.; Mohamed, I.A.A.; Khatab, A.; Sherif, A.; Wang, Z.; Salah, A.; Nishawy, E.; Ayaad, M.; Kuai, J.; et al. Modulation of Salinity Impact on Early Seedling Stage via Nano-Priming Application of Zinc Oxide on Rapeseed (*Brassica napus*, L.). *Plant Physiol. Biochem.* **2021**, *166*, 376–392. [CrossRef] [PubMed]

80. Marschner, H. *Mineral Nutrition of Higher Plants, 2nd ed*; Academic Press Pub.: New York, NY, USA, 1995; p. 559.

81. Gasic, K.; Korban, S.S. Expression of Arabidopsis phytochelatin synthase in Indian mustard (*Brassica juncea*) plants enhances tolerance for Cd and Zn. *Planta* **2007**, *225*, 1277–1285. [CrossRef]

82. Empadinhas, N.; Costa, M.S.d. Osmoadaptation mechanisms in prokaryotes: Distribution of compatible solutes. *Int. Microbiol.* **2008**, *11*, 151–161. [CrossRef] [PubMed]

83. Magnaval, C.; Noirot, M.; Verdeil, J.; Blattes, A.; Huet, C.; Grosdemange, F.; Buffard-Morel, J. Free amino acid composition of coconut (*Cocos nucifera* L.) calli under somatic embryogenesis induction conditions. *J. Plant Physiol.* **1995**, *146*, 155–161. [CrossRef]

84. George, E.F.; Hall, M.A.; De Klerk, G.J. *Plant Propagation by Tissue Culture*, 3rd ed.; Springer: Dordrecht, The Netherlands, 2008; p. 107.

85. Bhaduri, A.M.; Fulekar, M.H. Antioxidant enzyme responses of plants to heavy metal stress. *Rev. Environ. Sci. Biotechnol.* **2012**, *11*, 55–69. [CrossRef]

86. Koç, E.; İşlek, C.; Büyükkartal, H.N. Comparison of phenylalanine ammonia lyase response to lead and zinc stress in different wheat genotypes. *Commun. Fac. Sci. Univ. Ank. Ser. C* **2018**, *27*, 37–44.

87. Farghaly, F.A.; Radi, A.A.; Al-Kahtany, F.A.; Hamada, A.M. Impacts of zinc oxide nano and bulk particles on redox-enzymes of the Punica granatum callus. *Sci. Rep.* **2020**, *10*, 19722. [CrossRef]

88. Asada, K. Production and action of active oxygen species in photosynthetic tissues. In *Causes of Photo-Oxidative Stress and Amelioration of Defense Systems in Plants*; Foyer, C., Mullineaux, P., Eds.; CRC Press: Boca Raton, FL, USA, 1994; pp. 77–104.

89. Rai, V.; Vaypayee, P.; Singh, S.N.; Mehrotra, S. Effect of chromium accumulation on photosynthetic pigments oxidative stress defence system nitrate reduction proline level and eugenol content of *Ocimum tenuiflorum* L. *Plant Sci.* **2004**, *167*, 1159. [CrossRef]

90. Radi, A.A.; Farghaly, F.A.; Al-Kahtany, F.A.; Hamada, A.M. Zinc oxide nanoparticles-mediated changes in ultrastructure andmacromolecules of pomegranate callus cells. *Plant Cell Tissue Organ Cult.* **2018**, *135*, 247–261. [CrossRef]